Applied Acoustics 255 (2027) 111526

Contents lists available at ScienceDirect

Applied Acoustics

journal homepage: www.elsevier.com/locate/apacoust

Tonal noise generation from tandem cylinders of unequal diameter in cross-flow☆

Thomas F. Geyer[a,*], Paul Abromeit[b], Maximilian Prügel[b], Sparsh Sharma[c], Lars Enghardt[d]

[a] German Aerospace Center, Institute of Electrified Aero Engines, Department of Environmental Impact and Sensor Technology, Lieberoser Str. 13 A, Cottbus, 03046, Germany
[b] Brandenburg University of Technology, Chair of Electrified Aero Engines, Lieberoser Str. 13 A, Cottbus, 03046, Germany
[c] German Aerospace Center, Institute of Aerodynamics and Flow Technology, Lilienthalplatz 7, Braunschweig, 38108, Germany
[d] German Aerospace Center, Institute of Electrified Aero Engines, Lieberoser Str. 13 A, Cottbus, 03046, Germany

HIGHLIGHTS

- Flow around tandem cylinders of unequal diameter in a crossflow generates tonal noise.
- This noise scales with the the upstream cylinder diameter when the upstream cylinder thicker than the downstream cylinder.
- When the downstream cylinder is thicker and for small spacings, the tonal noise scales with the downstream cylinder diameter.
- The directivity of the dominant tonal peak in the far-field suggests a classical dipole radiation pattern.

ARTICLE INFO

Keywords:
Tandem cylinder flow noise
Vortex shedding
Aeroacoustic wind tunnel

ABSTRACT

The flow around two parallel cylinders arranged in a tandem configuration is a major source of aerodynamically induced noise and vibrations that can be found in a variety of technical applications. Although this configuration has already been the subject of many past investigations, the effect of unequal cylinder diameters on the resulting far-field tonal noise has not been fully addressed yet, especially for varying streamwise distances between the two cylinders. The present paper describes an experimental acoustic study on tandem cylinder configurations with varying diameters and normalized spacings, where special emphasis was placed on the identification of basic scaling approaches. Additional two-dimensional flow simulations were performed to enable a better qualitative understanding of the flow phenomena. The resulting dataset shows that in most cases, the vortex shedding tonal noise scales with the upstream cylinder diameter. However, for small spacings and large ratios of downstream cylinder diameter to upstream cylinder diameter, the vortex shedding scales with the downstream cylinder diameter. The dominant tonal peak essentially shows a classical dipole-like directivity.

1. Introduction

The generation of aerodynamic noise by two cylinders placed in a tandem configuration is a classical problem in aeroacoustics, as it constitutes a simple model for parts of the aircraft landing gear, protective guard grilles for axial fans, overhead power lines, offshore wind energy farms, cables in cable-stayed long-span bridges as well as pipes in heat exchangers. Subsequently, various research has been performed on such configurations. One early overview of aerodynamic studies on flow around a pair of parallel cylinders was given by Zdravkovich [1]. For cases with two cylinders in a streamwise line without an angle of incidence, which constitutes the classical tandem cylinder configuration, the work cites the reports from Igarashi [2,3]. It is summarized in [1] that for spacings up to some critical value around 3.5 to 4 cylinder diameters D, the vortex shedding from the upstream cylinder is suppressed, while for larger spacings both cylinders individually develop vortex streets. The proximity region can be subdivided into further regions: For very small spacings below $1.1D$, both cylinders behave as one bluff body.

☆ Part of the results from this paper have been shown as paper 3212 in the 2025 AIAA Aviation Forum and Ascend.

* Corresponding author.
Email addresses: thomas.geyer@dlr.de; thomas.geyer@b-tu.de (T.F. Geyer).

https://doi.org/10.1016/j.apacoust.2026.111526
Received 13 March 2026; Received in revised form 11 June 2026; Accepted 14 August 2026
Available online 28 August 2026

For spacings approximately between 1.1 and 1.6D, an alternate reattachment of the shear layers takes place on the windward side of the downstream cylinder, while for larger spacings of up to 2.4 diameters, quasi-steady reattachment of the separated shear layers is observed on the downstream cylinder. For spacings greater than 2.5D up to the critical spacing, the reattachments are occasionally disrupted, but still no regular vortex shedding from the upstream cylinder occurs. Around the critical distance, a bistable range is located. For spacings larger than the critical range, both cylinders form individual vortex streets. The review focuses on cylinder oscillations, and hence no statements are made on the resulting aerodynamically induced far-field noise.

The early studies by Hiwada et al. [4] and Igarashi [5], the results of which are included in the comprehensive review by Zdravkovich [6], focus on the flow around two circular cylinders of unequal diameter. The review paper [6] differentiates between three cases: The first is that the thinner cylinder is placed upstream and the thicker downstream, the second is that the thinner cylinder is placed downstream from the thicker one and the third describes the special case of a very thin cylinder (labeled “control cylinder”) used for flow control around a thicker cylinder. For the first case it is stated that for small distances the shear layers from the thinner upstream cylinder do not roll up, but stretch towards the thicker downstream cylinder, while for larger spacings the shear layers from the upstream cylinder will roll up and form typical von-Kármán vortices [4]. A linear relationship is given for the respective spacing at which this behavior switches between the two states. For the second case, where the upstream cylinder has a larger diameter than the downstream cylinder, it was found that the dependence of the flow patterns on the normalized spacing is similar to that observed for the classical tandem case with two cylinders of equal diameter (although the individual flow fields are notably different for small spacings). This includes, first, a very close region where the shear layers of the upstream cylinder do not reattach on the downstream cylinder, followed by regions where reattachment happens. Around the critical distance, bistable flow patterns can be observed. At larger spacings, the shear layers from the upstream cylinder roll up and start to form individual vortices in the region between the two cylinders.

A configuration of two cylinders of equal diameter, with a streamwise separation of 3.7 cylinder diameters, serves as an aeroacoustic benchmark problem for parts of the landing gear of aircraft [7,8]. Thus, a substantial number of experimental and numerical results are available for this selected case, for example [9–12].

A very detailed experimental investigation on the flow around two parallel cylinders in various staggered arrangements was provided by Hu and Zhou [13,14]. Depending on the angle of incidence and the distance between the cylinders, they identified four distinct flow modes. Another fundamental experimental aerodynamic study of the flow around two circular cylinders of equal diameter in various arrangements, including the case of tandem cylinders, was performed by Sumner et al. [15]. They provide detailed data on aerodynamic force coefficients, Strouhal numbers, and spectra of velocity fluctuations for different configurations in the subcritical Reynolds number regime. Experimentally obtained steady and unsteady forces acting on cylinders in two tandem configurations with different spacing are given in the work of Schewe et al. [16] especially for very high Reynolds numbers. Due to the complexity of the flow field depending on the flow regime and the details of the configuration, there are a variety of studies, some of them quite recent, that provide high-quality flow simulations around two cylinders and hence improve the understanding of the physical mechanisms, such as [17,18].

Many studies focus especially on vortex-induced vibrations, as they are known to have a high potential for structural damage. One such investigation is the work of Mittal and Kumar [19], who analyzed vortex-induced vibrations of tandem cylinders at a large cylinder spacing of 5.5 diameters numerically. Several other numerical analyses of flow-induced vibrations of two cylinders in tandem and staggered arrangements are available in the literature, e.g., [20,21], confirming the importance of the problem. Experimental data from measurements on tandem and staggered configurations in a water tunnel were provided by Assi [22].

A comprehensive overview of aerodynamic studies on a pair of cylinders in a cross-flow is given by Sumner [23], including a detailed discussion of the flow patterns depending on cylinder distance and flow incidence. In addition, it must be mentioned that tandem cylinder configurations have also been used to study the noise reduction capabilities of porous cylinder coatings, both numerically [24,25] and experimentally [26,27].

As can be seen from several of the above-mentioned studies, in addition to the standard configuration of two cylinders of equal diameter placed at an angle of zero degrees to the incoming flow, research has also focused on the influence of parameters like the angle of incidence between the cylinders [15,28,29]. Another special case of interest is the configuration consisting of two parallel circular cylinders with different diameters. Several studies have been performed that focus on the flow structures and wake dynamics around the cylinders [30–32]. In addition, this configuration can also lead to severe vortex-induced vibrations, and hence potential damage [33].

However, currently there is only a very limited number of studies on the aerodynamic noise generation by such a configuration with unequal cylinder diameters. Existing investigations include the fundamental work by Hutcheson and Brooks [34], which contained the cases of a cylinder with a diameter of 25.4 mm placed upstream and one with a 12.7 mm diameter placed downstream and vice versa. They were placed with a fixed spacing of three times the larger diameter. It was found that the far-field noise spectra displayed a peak at a frequency roughly corresponding to the von-Kármán vortex shedding frequency of the upstream cylinder. Another, more recent study is that by Mg and Jothi [35], who performed measurements on tandem cylinders with three different diameter ratios of 0.4, 1, and 2.5 (referring to the ratio of the upstream cylinder diameter to the downstream cylinder diameter). The spacing between the cylinders was two and four diameters, referring to the larger cylinder. They found that, for the smaller cylinder spacing, the tonal noise is generated by vortices being shed from the downstream cylinder, while for the larger spacing two tonal peaks are visible in the case when the thinner cylinder was upstream and only one tone was visible when the thicker cylinder was upstream, corresponding to the vortex shedding from the upstream cylinder. First results of the current study [36] for a tandem cylinder configuration using two cylinders of 18 mm and 30 mm in diameter, respectively, showed that for a spacing of 3.7 diameters (referring to the diameter of the thicker cylinder), the vortex shedding is governed by the upstream cylinder. These results were qualitatively confirmed using two-dimensional Computational Fluid Dynamics simulations. This shows that, although some data are available on the aerodynamic noise generated by a tandem cylinder configuration with two circular cylinders of unequal diameter, they are very limited with respect to the diameter ratios and the cylinder spacings. In particular, the question regarding the origin of the vortex shedding tonal noise (either coming from the upstream cylinder or from the downstream cylinder) is not fully answered. Thus, the present paper aims to provide a more comprehensive data set, including a larger set of cylinders at a variety of cylinder spacings in the sub-critical Reynolds number regime. Besides the presentation of far-field sound data, possible scaling approaches will be discussed, aided by qualitative two-dimensional flow simulations.

The remaining part of the paper is structured as follows: In Section 2, the experimental setup is detailed, including the wind tunnel facility, the cylinder models and the acoustic measurement technique. In addition, the setup of the two-dimensional flow simulations is described briefly. In the following Section 3, results are presented and discussed, including an investigation of possible scaling laws for the vortex shedding tonal noise of the configurations. Finally, the findings are summarized in Section 4.

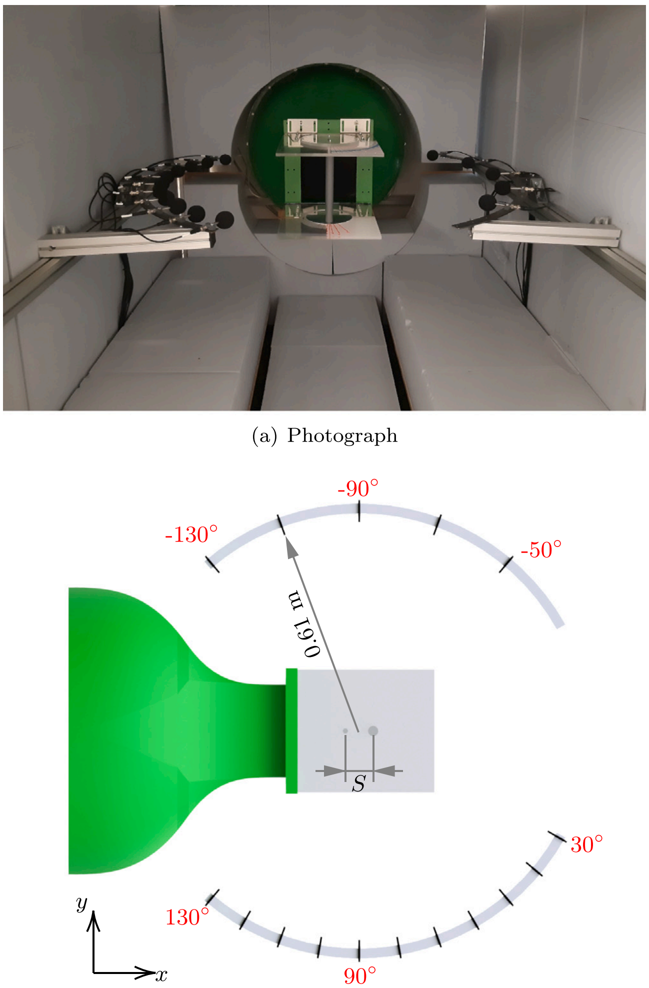

(a) Photograph

(b) Schematic (top view)

Fig. 1. Experimental setup in the aeroacoustic wind tunnel facility.

2. Experimental and numerical setup

2.1. Wind tunnel

All experiments were performed in the small aeroacoustic open jet wind tunnel at the Brandenburg University of Technology [37], using a nozzle with a rectangular exit area of 0.28 m (height) × 0.23 m (width). Attached to the nozzle were two side plates made of acrylic glass, to which the cylinders were affixed. In the experiments, the distance between the center of the cylinders and the nozzle exit was kept constant at 0.18 m for each cylinder spacing, which means that for large spacings S between the cylinders the upstream cylinder was closer to the nozzle than for smaller spacings. The test section of the wind tunnel is lined on four sides with sound absorbing foam, leading to a quasi-anechoic measurement environment at frequencies above approximately 125 Hz. Fig. 1 shows a photograph and a schematic of the experimental setup. The turbulence intensity of the flow at a downstream distance of 0.15 m from the nozzle is about 0.25 % at a flow velocity of 20 m/s [38].

In the present study, acoustic measurements were performed at four different flow velocities U_0 of approximately 15 m/s, 20 m/s, 30 m/s, and 40 m/s, corresponding to Mach numbers $M = U_0/c$ (with c being the speed of sound) of 0.04, 0.06, 0.09, and 0.12, respectively.

2.2. Tandem cylinder configurations

In total, six different cylinder models were used in the study. They all had the same length l of 0.28 m, but varied in diameter from 6 mm to 40 mm. These cylinders have been used in prior studies in the same facility [38,39]. They lead to a wind tunnel blockage of less than 18 % (wind tunnel blockage being the main limit for the maximum cylinder diameter). Two different general setups were examined in this study: The first one comprised configurations where the diameter D of the downstream cylinder was kept constant at 30 mm, while the diameter of the upstream cylinder, d_u, was varied. In the second case, the upstream cylinder had a fixed diameter $D = 30$ mm, while the downstream cylinder diameter, d_d, was varied. This led to different ratios d_u/D and d_d/D from 0.2 to 1.33, which are specified in Table 1, as well as to different ratios d_u/d_d. The resulting aspect ratio l/d of the single cylinders takes values between 7 and 47. Thus, periodic von-Kármán vortex shedding can be expected [40].

Table 1
Diameters of the tandem cylinders used in the present study (note that the diameters d_u, d_d of the upstream and downstream cylinders vary while the diameter D of the other cylinder remains constant).

Variation of the upstream cylinder diameter			
Upstream cylinder diameter d_u (mm)	downstream cylinder diameter D (mm)	cylinder length l (mm)	d_u/D
6	30	280	0.2
10	30	280	0.33
15	30	280	0.5
20	30	280	0.67
30	30	280	1.0
40	30	280	1.33
Variation of the downstream cylinder diameter			
Upstream cylinder diameter D (mm)	downstream cylinder diameter d_d (mm)	cylinder length l (mm)	d_d/D
30	6	280	0.2
30	10	280	0.33
30	15	280	0.5
30	20	280	0.67
30	30	280	1.0
30	40	280	1.33

In addition, the streamwise spacing between the two cylinders S was varied, taking values of $S/D = 1.7$, 2.7, 3.7, 4.7, and 5.7. These normalized spacings were mainly chosen as they represent typical flow regimes for cylinders in tandem arrangement [1]: Two spacings are located in the proximity region ($S/D = 1.7$ and 2.7), one corresponds approximately to the critical spacing while also corresponding to the benchmark configuration ($S/D = 3.7$) [7,8] and two are located in the wake interference region, where individual vortex shedding from both cylinders is expected ($S/D = 4.7$ and 5.7). Using the benchmark spacing additionally allows for comparison of the results with those from previous studies by the authors [26,27]. The rationale for selecting exactly these values was based on the desire to include the benchmark spacing as well as on the idea to have integer steps between the selected spacings. Of course, a finer resolution of cylinder spacings would probably provide a better understanding of the flow-acoustic phenomena, but that was not possible within the framework of the present study, leaving room for future experiments on selected spacings not covered here. It should be noted that different notations would generally be possible, for example the nondimensionalization of the spacing with either the upstream cylinder (as done in [4]) or the downstream cylinder.

Based on the nominal diameter D of 30 mm, the resulting Reynolds number range is from approximately $Re = 30{,}000$ to 80,000. When the Reynolds number is calculated based on the upstream cylinder diameter, the Reynolds number ranges from 6000 to 106,000. These ranges correspond to the sub-critical flow regime [41], which is characterized by a laminar near-wake with transition in the shear layers and periodic vortex shedding from the cylinder.

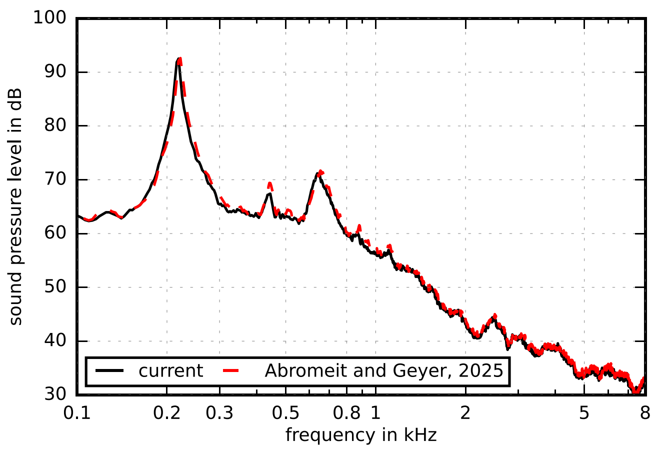

Fig. 2. Comparison of sound pressure level spectra obtained by a microphone located at 90° to the flow at a flow speed of approximately 40 m/s for the configuration of two cylinders of equal diameter (D = 30 mm) at a normalized spacing of S/D = 3.7 in the present study with results for the same configuration from an earlier study [27].

2.3. Acoustic measurements and data analysis

The acoustic measurements were performed using 16 1/4 in. free-field measurement microphones positioned on two arcs with a radius of 0.61 m, located on opposite sides of the test section. This is shown in detail in the schematic in Fig. 1(b). The microphone arc shown on the bottom side in Fig. 1(b) contains eleven microphones with a spacing of 10°, while the arc on the other side contains five microphones with a spacing of 20°. The microphones have a nominal sensitivity of 50 mV/Pa and a typical frequency response of ±0.5 dB in a frequency range from 20 Hz to 4 kHz. They were calibrated at a single tone (frequency 1 kHz, amplitude 1 Pa) with a calibrator. Acoustic time-data were recorded with a sampling frequency of 51.2 kHz and a duration of 60 s. In post-processing, which was performed using the open-source software package *Acoular* [42], the data were transferred to the frequency domain using a Fast Fourier Transform (FFT) on blocks of 16,384 samples with an overlap of 50 % and the Hanning window function.

In order to assess the repeatability of the experimental procedure, Fig. 2 presents a comparison of two measurements on the reference configuration (both cylinders have the same diameter of D = 30 mm) with a spacing of 3.7D, which were taken under comparable conditions in the same facility. The first measurement was taken as part of the current study, while the second was part of a study on porous-coated staggered cylinders published by the authors [27]. The results agree very well, with sound pressure level differences in the frequency range of interest in the order of 1 dB. The frequency of the vortex shedding peak differs by 3.125 Hz, which corresponds to the frequency resolution of the FFT. This essentially confirms the high accuracy of the measurements performed.

The majority of analyses presented in the current paper are performed for data obtained with the microphone on the bottom arc in Fig. 1 which is located at 90° to the flow. As the tonal noise generated by vortex shedding at the cylinders can be assumed to feature a classical dipole noise source directivity, this microphone location is aligned with the direction of maximum noise radiation. In addition, noise directivity effects are discussed based on results from all eleven microphones located on this arc.

2.4. Flow simulations

In order to enable an easier interpretation of the experimental acoustic results, two-dimensional incompressible flow simulations for non-reactive flow were performed using an open-source Computational Fluid Dynamics (CFD) code [43]. The code solves the incompressible continuity and Navier–Stokes equations using a fractional-step (pressure-correction) method, in which the momentum equation is first advanced without the pressure term and the resulting divergence error is subsequently corrected by solving a Poisson equation for the pressure. Spatial derivatives are approximated with a fourth-order central finite-difference scheme combined with a Lax–Wendroff-type second-order time integration, providing a balance between accuracy and computational efficiency for qualitative flow visualization. The Poisson equation is solved iteratively using the Successive Over-Relaxation (SOR) method with a relaxation parameter of $\omega = 1.8$ and a convergence tolerance of $\epsilon_p = 1 \times 10^{-3}$, with a maximum of 200 iterations per time step. A second-order explicit spatial filter with a relaxation parameter of $\omega_{\mathrm{fil}} = 0.05$ was applied every time step to suppress numerical oscillations.

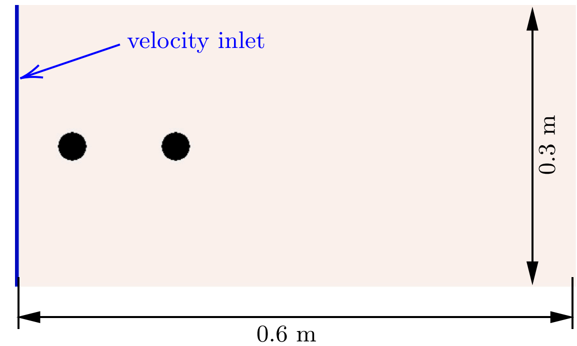

Fig. 3. Computational domain used for the two-dimensional flow simulation (configuration with S/D = 3.7, d_u = d_d =30 mm, blue color denotes inflow boundary, black color denotes non-slip boundary).

The computational domain, shown exemplarily in Fig. 3 for the configuration with two cylinders of equal diameter at S/D = 3.7, consists of 600 × 300 grid points. This corresponds to a physical extent of 0.6 m × 0.3 m in the streamwise and cross-stream directions, respectively, yielding a uniform grid spacing of Δx = Δy = 1 mm. The streamwise direction is denoted as x and the cross-stream direction as y. On the left boundary of the computational domain, a uniform velocity inlet boundary condition with U_0 = 40 m/s (streamwise component) and V = 0 m/s (cross-stream component) was imposed (Dirichlet condition for velocity, Neumann condition for pressure). Outflow boundary conditions (Neumann for velocity, Dirichlet for pressure set to the reference atmospheric pressure) were applied at the remaining boundaries of the domain. The cylinder surfaces were defined as no-slip (wall) boundary conditions, with zero velocity imposed at the wall. The atmospheric pressure in the domain was set to 1 × 10^5 Pa and the fluid density and dynamic viscosity were set to ρ = 1.2 kg/m^3 and μ = 2 × 10^{-5} kg/(m s), respectively, corresponding to standard air conditions. Each simulation was run for a total of 14,000 time steps, with the first 8000 time steps discarded to eliminate transient effects, so that the flow visualizations presented in the current work are based on the statistically developed flow field. The time step size was dynamically controlled by the CFL (Courant-Friedrichs-Lewy)-based criterion with a factor of 10.

It should be noted that these simulations are not intended to provide quantitative data, but rather to give a qualitative visualization of the vortex shedding processes associated with the different tandem cylinder configurations. In particular, the two-dimensional nature of the simulations and the relatively coarse representation of the cylinder geometry on the Cartesian grid preclude a direct quantitative comparison with the experimental acoustic results.

3. Results

In this section, the results of the acoustic measurements will be presented, while the corresponding discussion will be aided by the results from the 2D flow simulations.

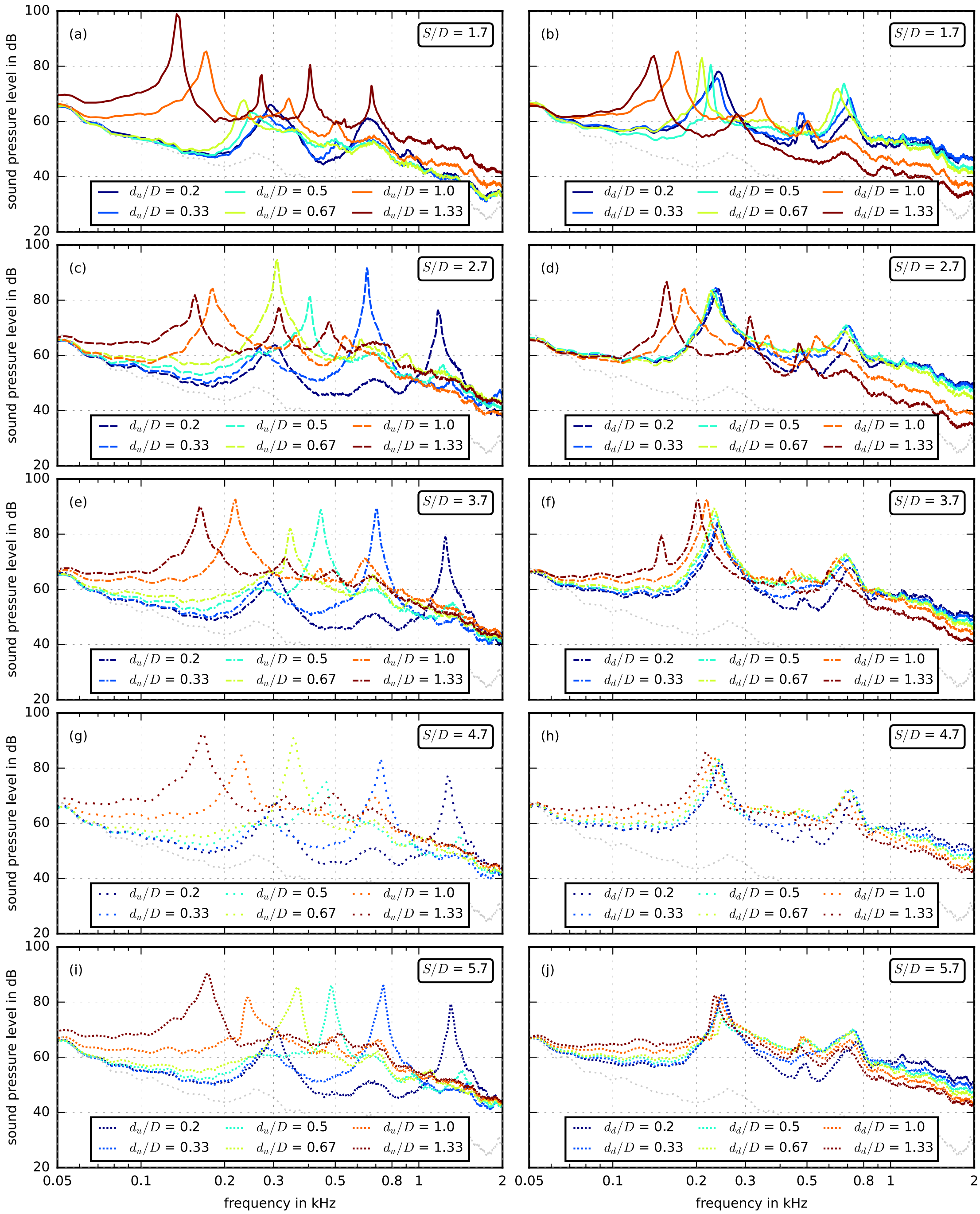

Fig. 4. Example sound pressure level spectra obtained by a microphone located at 90° to the flow at a flow speed of approximately 40 m/s ($M = 0.12$), left column: variation of the upstream cylinder diameter, right column: variation of the downstream cylinder diameter (gray dotted line: wind tunnel background noise).

3.1. Far-field sound pressure level spectra

In order to obtain a first understanding of the effect of different parameter variations on the resulting far-field sound, Fig. 4 shows example sound pressure level spectra obtained by the single microphone at an angle of 90° to the flow as a function of frequency. All geometrical variations (e.g., all spacings and all diameter variations) are included, but only one flow velocity of approximately 40 m/s was chosen, corresponding to a Mach number of 0.12 and a Reynolds number Re (based on the nominal diameter $D = 30$ mm) of 80,000. These results already reveal some interesting trends: In general, configurations where the upstream cylinder is varied (Fig. 4(a), (c), (e), (g), and (i)) show notable differences in the frequency of the vortex shedding peak for normalized spacings of $3.7D$, $4.7D$ and $5.7D$, indicating that the vortex shedding is governed by the diameter of the upstream cylinder at these spacings. For the configurations with spacings of $1.7D$ and $2.7D$ it appears that for larger diameter ratios ($d_u/D \geq 1$) the upstream cylinder governs the vortex shedding, too. Interestingly, the spectra of these configurations show a number of sharp tonal peaks with comparable amplitude. For smaller d_u/D, the spectra are notably different, although comparable to each other, indicating that the dominant noise generation mechanism is different. This indicates that for the smallest spacing, depending on the diameter ratio, the flow behavior might switch from a state in which the shear layers from the upstream cylinder stretch towards the downstream cylinder to one where the shear layers roll up, as was described in [4,6].

For the configurations where the upstream cylinder has a constant diameter of $D = 30$ mm and the diameter of the downstream cylinder d_u is varied (Fig. 4(b), (d), (f), (h), and (j)), the trends are very different for each spacing, indicating that the spacing has a greater effect on tonal noise generation. For small spacings of $1.7D$ and $2.7D$ (Fig. 4(b) and (d)), the differences in peak frequency indicate that the downstream cylinder influences the tonal noise due to vortex shedding. According to [5], it would be expected that the flow at this spacing is synchronized (at $S/D = 1.7$) and even features a quasi-stationary vortex (at $S/D = 2.7$), but with reattachment in both cases. However, as the tonal peaks observed for these spacings appear at different frequencies, at least for larger diameters of the downstream cylinder (large ratios of d_d/D), the far-field noise is apparently not caused by synchronized flow governed by the upstream cylinder, but by flow patterns governed by the downstream cylinder. Starting with the critical spacing of $3.7D$ (Fig. 4(f)) and, even more pronounced, for large spacings of $4.7D$ and $5.7D$ (Fig. 4(h) and (j)), the spectral shapes seem to be less affected by d_u. Although it is known that for large spacings above the critical spacing both cylinders will shed vortices independently [1], it appears that this does not lead to an individual sound propagation from both cylinders into the far-field with clearly distinguishable individual tones. It is likely that the main peak visible in the spectra is caused by the impingement of the vortex street from the upstream cylinder on the downstream cylinder.

With the aim of focusing on the sole effect of the cylinder spacing, independent of diameter variations, sound pressure level spectra of the configurations consisting of two cylinders of equal diameter ($d_u = d_d = D = 30$ mm) at all spacings investigated ($S = 1.7D$, $2.7D$, $3.7D$, $4.7D$, $5.7D$) are shown in Fig. 5. This is done for the same microphone at 90° to the flow and for the same flow velocity of approximately 40 m/s. Now, the spectra are presented as a function of the Strouhal number based on D. It is visible that a decrease in spacing leads to an increasing shift of the vortex shedding tone towards lower Strouhal numbers, and, at the same time, to a decrease in broadband noise. This shift is probably caused by a reduction in the mean velocity, when the downstream cylinder is located in the wake of the upstream cylinder. In addition to the peak Strouhal number, the spacing also affects the level of the tonal peak. However, this does not seem to be governed by an equally simple trend, as the maximum level is obtained for the configuration with $S/D = 3.7$, which is also covered in the NASA benchmark [7]. It should again be noted that the region with normalized distances S/D between roughly 3 and 4 is described as the critical spacing, where the wake characteristics change from a single vortex street to individual vortex streets from both cylinders and a bistable behavior can be expected [1]. In addition, Fig. 5 also includes the far-field noise generated by a single cylinder with $D = 30$ mm. The tonal noise peak due to vortex shedding is visible at a Strouhal number of approximately 0.19, which agrees well with values from the literature (e.g., [34]), while smaller peaks are visible at two and three times this Strouhal number. It is known from theory [44] that the main peak is caused by fluctuating lift forces acting on the cylinder and the second by fluctuating drag forces. At spacings above the critical one ($S/D = 4.7$ and 5.7), the resulting tonal peaks basically resemble those of the single cylinder. This agrees with the theory that both cylinders form individual vortex streets at these spacings, which would lead to an identical (but not necessarily synchronized) generation of tonal vortex shedding noise.

In order to obtain a better understanding of the dependence of the tonal noise generation on the ratio of the cylinder diameters, Fig. 6 shows a subset of the results from Fig. 4, concentrating on only two cylinder diameters at the critical spacing of $3.7D$. It contains the reference configuration with $d_u = d_d = D = 30$ mm as well as a selected configuration with a thinner upstream cylinder ($d_u = 10$ mm, $d_d = D = 30$ mm) and one with a thinner downstream cylinder ($d_u = D = 30$ mm, $d_d = 10$ mm). In addition, corresponding spectra obtained for single

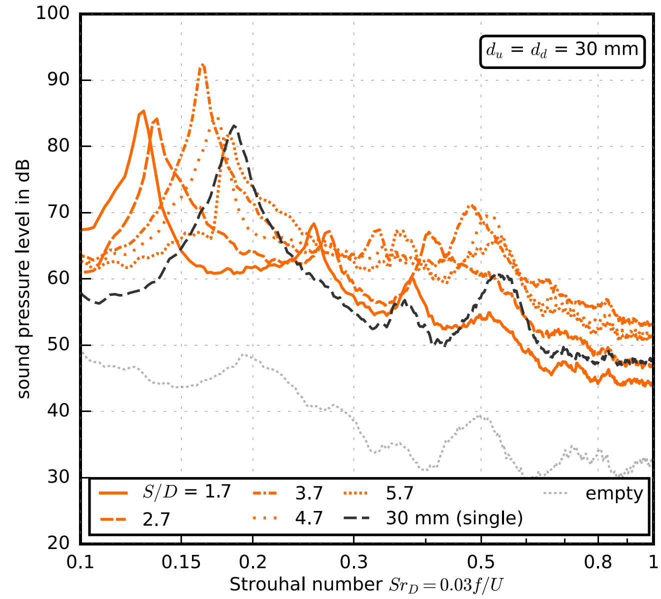

Fig. 5. Sound pressure level spectra obtained by a microphone located at 90° to the flow at a flow speed of approximately 40 m/s ($M = 0.12$) for the configurations with equal cylinder diameters at different spacings.

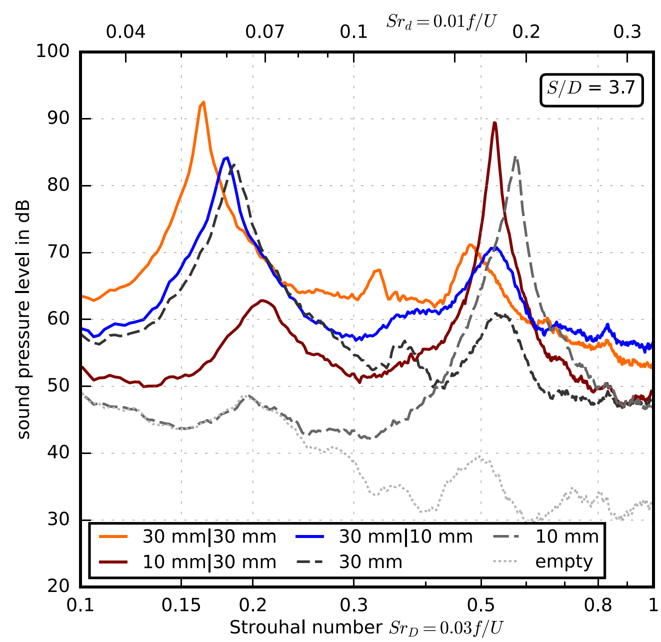

Fig. 6. Sound pressure level spectra obtained by a microphone located at 90° to the flow at a flow speed of approximately 40 m/s ($M = 0.12$) for two configurations with unequal cylinder diameters at $S = 3.7D$.

cylinders with diameters of 10 mm and 30 mm are included. It becomes immediately evident that at this cylinder spacing, the vortex shedding tonal noise is apparently governed by the upstream cylinder, as the configuration with the thinner cylinder at the upstream position leads to a tonal peak at a high frequency, which is in the same frequency range as the peak observed for the single thin cylinder. In addition, a second, much lower and broader peak is visible at a Strouhal number Sr_D (based on the larger cylinder diameter) around 0.2. In the early work of Hiwada et al. [4], the spacings for configurations with a thinner upstream cylinder are scaled with the upstream cylinder, which in the present case would lead to a much larger spacing of $S/d > 10$. Such a large spacing indicates individual vortex shedding from both cylinders, which explains the two peaks observed in the spectra. However, as the peak attributed to the upstream cylinder has an amplitude that is more than 25 dB above the peak attributed to the downstream cylinder, the vortex shedding tonal noise propagation is clearly dominated by the flow around the upstream cylinder. This agrees with the findings observed in [35]. The low amplitude of the tonal noise attributed to the thicker downstream cylinder may also be affected by the fact that the mean velocity is lower in the wake of the upstream cylinder, leading to a reduction in the acoustic source strength.

The configuration with the thin cylinder downstream, on the other hand, leads to a tonal peak at a much lower frequency, which is more aligned with the reference configuration as well as the single thick cylinder. However, a slight shift towards lower Strouhal numbers compared to the reference configuration is still visible. This agrees with previous results reported for the tandem cylinder benchmark case [8]. As this spacing belongs to the critical region, where a bistable behavior can be expected [1] and the shear layers roll up in front of the downstream cylinder [5], such small differences are not exactly unexpected. In addition, it has to be noted that a scaling with a different dimension than the diameter of the cylinders is possible. Gennaro et al. [45], for example, state that a scaling with a wake parameter, such as the wake width, is better suited for the scaling of vortex shedding noise from single cylinders. However, additional flow field measurements would be necessary in order to test this hypothesis for the configurations considered in the present work.

In an attempt to examine the effect of the Reynolds number on the resulting far-field noise, Fig. 7 shows sound pressure level spectra obtained with the microphone at 90° to the flow for the configurations examined in Fig. 6 with two unequal cylinder diameters (d_u = 10 mm, $d_d = D$ = 30 mm and $d_u = D$ = 30 mm, d_d = 10 mm) for all four flow velocities adjusted in the present study (U_0 = 15 m/s, 20 m/s, 30 m/s and 40 m/s). Based on the nominal cylinder diameter D = 30 mm, this corresponds to Reynolds numbers of approximately 30,000, 40,000, 60,000 and 80,000, respectively. In addition, Fig. 7 is divided into three individual plots: Fig. 7(a) shows spectra for configurations with the smallest spacing of S/D = 1.7, Fig. 7(b) those for the medium (critical) spacing of S/D = 3.7 and Fig. 7(c) those for the largest spacing of S/D = 5.7. For the latter two spacings (Fig. 7(b) and (c)), the basic trends are very similar. With increasing velocity, the dominant peaks in the far-field spectra increase in amplitude and shift towards lower Strouhal numbers. This includes both the configurations with the thinner upstream cylinder, which tend to scale with the smaller diameter, as well as the configurations with the thicker upstream cylinder, for which the tonal noise is apparently also governed by the upstream cylinder. An increase in amplitude would be expected, as the sound power of a typical dipole noise source scales with the sixth power of the flow speed ($P \propto U^6$). With respect to the peak Strouhal number, the values shift from approximately 0.22 at the lowest Reynolds number to 0.18 at the highest Reynolds number for both configurations at the highest spacing (and similar values can be seen for the critical spacing). Such variations of the vortex shedding Strouhal number with Re have also been observed in experimental investigations on single cylinders [34,38] and can be explained by the classical $Re - Sr$-dependency of flow around circular cylinders [46,47].

At the smallest spacing, the dependency on Reynolds number is basically similar, although the assignment of the peaks to vortex shedding from each of the cylinders is more complex (which has already been observed in Fig. 4(a) and (b)). For the configuration with the thicker cylinder upstream (30 mm|10 mm), three tonal peaks are now visible in the far-field sound pressure level spectra. The highest peak is apparently governed by flow around the upstream cylinder, with the corresponding Strouhal number Sr_D changing from approximately 0.21 at the lowest Reynolds number to 0.18 at the highest, which can again be explained by the classical dependency of Strouhal number on Reynolds number in this flow regime. The second highest peak for most flow velocities can be

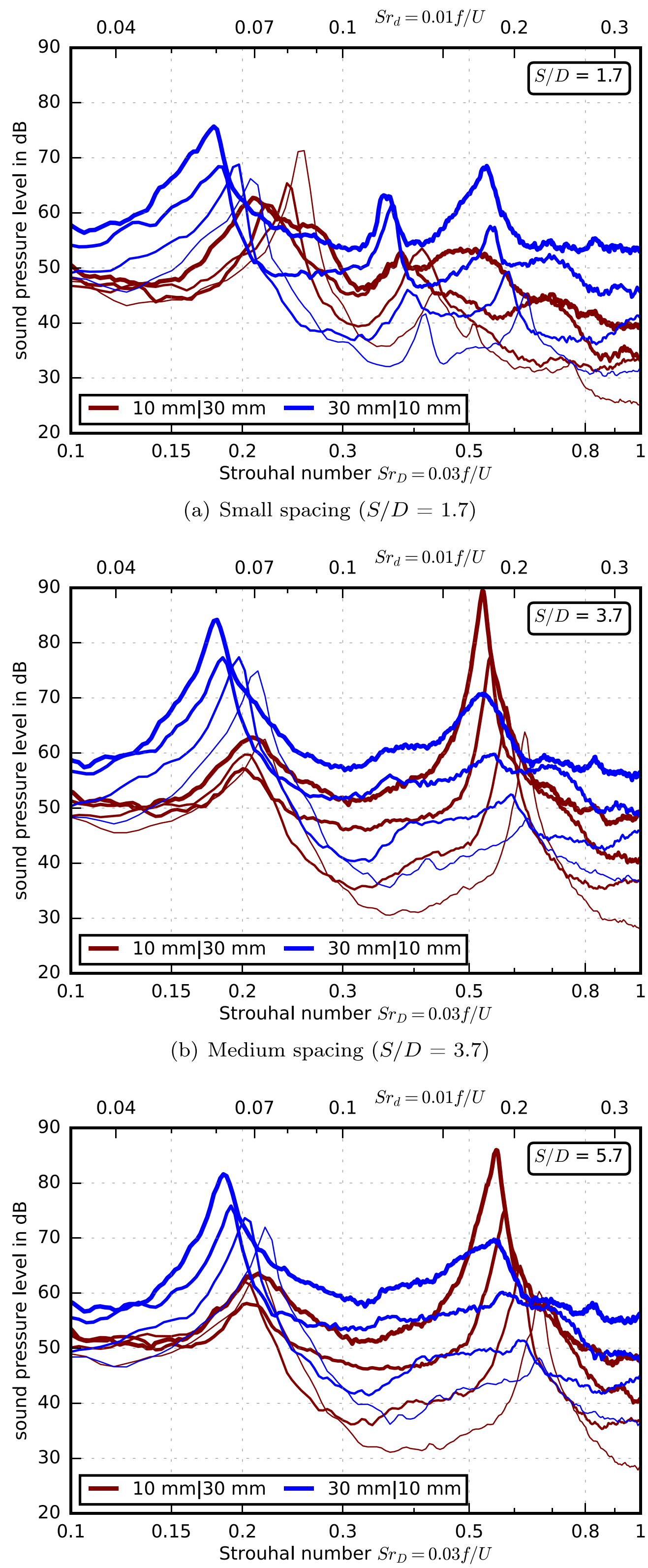

(a) Small spacing (S/D = 1.7)

(b) Medium spacing (S/D = 3.7)

(c) Large spacing (S/D = 5.7)

Fig. 7. Sound pressure level spectra obtained by a microphone located at 90° to the flow at flow speeds from 15 m/s to 40 m/s for two configurations with unequal cylinder diameters at three different spacings.

seen at Strouhal numbers that apparently are linked to the thinner downstream cylinder. This peak, however, is very sensitive with respect to Reynolds number, as its amplitude increases from approximately 45 dB to nearly 70 dB when the flow velocity is increased from 15 m/s to 40 m/s - a much stronger dependency then that of the first peak. The reason for this behavior is not fully clear yet, however, results from Igarashi [5] already show a Reynolds number-dependent change of flow regimes, characterized by different reattachment flow patterns, at such small spacings. The most interesting observation for this particular configuration, however, is the appearance of a third tonal peak in the far-field spectra, which can be seen at a frequency between that of the first peak (scaling with the thicker upstream cylinder diameter) and that of the second peak (scaling with the thinner downstream cylinder diameter). Similar to the second peak, the amplitude of this third peak shows a strong dependency on Reynolds number, whereas the shift in Strouhal number is similar to that of the other peaks. The physical noise generation mechanism of this peak is currently not clear - it could be some gap flow phenomenon connected to the separation distance of the two cylinders, for example. The emergence of this third peak should be analyzed in future studies using high-quality flow measurement techniques, such as Particle Image Velocimetry (PIV), or by performing 3D numerical flow simulations. The Reynolds number dependency of the second configuration, with the thinner cylinder upstream (10 mm|30 mm), is also very interesting for the case of the smallest spacing of $S/D = 1.7$. Here, the most dominant peak appears to be rather governed by the thicker downstream cylinder, but the peak amplitude decreases with increasing flow velocity. This effect is counterintuitive, as vortex-shedding induced noise would usually be expected to show a behavior related to a classical dipole source, which would dictate an increase in amplitude with velocity. It is possible, though, that the observed behavior has to do with an effect of the small upstream cylinders wake on the mean flow velocity that encounters the thicker downstream cylinder. Another interesting observation is that the peak frequency and the associated Strouhal number Sr_D are notably higher than that of the corresponding peak obtained for the configuration with the thinner cylinder located downstream (30 mm|10 mm). Again, a possible explanation is that the mean velocity of the flow interacting with the downstream cylinder is notably reduced due to the presence of the thin upstream cylinder, which would of course also affect the Strouhal number. Finally, it is also interesting to notice that the peak at the highest flow velocity ($U_0 = 40$ m/s) is much broader and seems to be merged with a second peak. These effects can currently not be analyzed in more detail without any high-resolution flow measurements or simulations. In addition, it should again be noted that in previous studies on configurations with a thinner upstream cylinder [4,6], the smaller diameter was taken as a reference dimension for the scaling of the spacing. In the present case, this would lead to a normalized spacing of $S/d = 5.1$, which would mean that both cylinders shed vortices independently. The fact that this does not explain the behavior observed in Fig. 7(a) for the configuration with the thinner cylinder upstream hints at differences between local flow phenomena in the direct vicinity of the cylinders and the tonal noise propagation into the far-field.

In the following subsection, classical scaling approaches based on the diameters of the two cylinders will be tested on the current dataset to obtain a better understanding of the shedding mechanisms, which will be complemented by qualitative results from 2D flow simulations.

3.2. Scaling

In the next step, the dependence of the main vortex shedding tonal peak on the parameters of the configuration will be further investigated. To this end, Fig. 8 shows two different Strouhal numbers: one that is calculated using the diameter of the upstream cylinder, $f\,d_u/U$ (Fig. 8(a)), and one that is calculated using the diameter of the downstream cylinder, $f\,d_d/U$ (Fig. 8(b)). In Fig. 8(a), results are presented as a function of the ratio of the upstream cylinder diameter to the downstream cylinder diameter, d_u/d_d, for all measured configurations and all flow velocities. In Fig. 8(b), the reciprocal ratio d_d/d_u has been used to enhance visibility.

It is visible from Fig. 8(a) that for large ratios of d_u/d_d (approximately $d_u/d_d \geq 2$), the Strouhal number based on the upstream cylinder diameter is approximately constant, with values between 0.17 and 0.22. This includes most of the configurations for which the upstream cylinder was kept constant ($d_u = D = 30$ mm) and the downstream cylinder was varied (right column in Fig. 4), revealing that the noise generation of the dominant tonal peak in these cases seems to scale with the thicker upstream cylinder. The resulting Strouhal numbers in this region still show a notable dependence on flow velocity, as the Strouhal number decreases with increasing velocity. This has been observed in more detail in Fig. 7 and, as discussed before, is not unexpected, as the vortex shedding Strouhal number of a single cylinder is known to depend on Reynolds number (see, for example, [34,38,46,47]).

Corresponding results from the 2D flow simulations for these configurations are shown in Fig. 9. These visualizations are based on the out-of-plane vorticity field, $\omega_z = \partial v/\partial x - \partial u/\partial y$, displayed using a red-to-blue color map, with red and blue indicating positive and negative vorticity, respectively. Due to the fact that the two largest spacings of the current study, $S/D = 4.7$ and $S/D = 5.7$, belong to the same flow regime (see Section 1) and to increase visibility for the remaining cases, results for $S/D = 5.7$ are not shown here.

It is visible that, although the smaller downstream cylinder can lead to small, but visible vortices that appear in the wake (see, for example, Fig. 9(d), (g), and (j)), the total, large-scale vortex street is still governed by the thicker upstream cylinder. Interestingly, the resulting flow visualization for the configuration with $d_u = d_d = 30$ mm at a normalized spacing of $S/D = 4.7$ shows a more chaotic behavior, although the main vortex pairs that form the Kármán vortex street are still visible. For small values of $d_u/d_d < 2$, no clear trends appear to be visible from Fig. 8(a). Especially for configurations with the smallest spacing of $S/D = 1.7$, a scaling of the vortex shedding tonal noise with the Strouhal number based on d_u does not seem to be a feasible assumption.

Now, when the Strouhal number is calculated based on the diameter d_d of the downstream cylinder as the characteristic dimension, and when this Strouhal number $f\,d_d/U$ is displayed as a function of the inverse diameter ratio, d_d/d_u, as shown in Fig. 8(b), the results obtained for large ratios d_d/d_u (corresponding to small values of $d_u/d_d < 2$) and the smallest spacing of $S/D = 1.7$ lead to approximately constant values around 0.2, which would be expected for single cylinders. Thus, this presentation of the current results reveals the tendency that the dominant tonal noise from tandem cylinder configurations with a thicker downstream cylinder at small cylinder spacings rather scales with the downstream cylinder. This is basically confirmed by the flow simulation results shown in Fig. 10: For small spacings of $S/D = 1.7$ (Fig. 10(a)–(c)) and $S/D = 2.7$ (Fig. 10 (d), (e), and (f)), the upstream cylinder appears to not lead to individual periodic von-Kármán vortex shedding, but instead the shear layers extend downstream and “wrap around” the downstream cylinder. For larger spacings, however, the upstream cylinder shows a clear vortex shedding street, which agrees well with the literature on tandem cylinder aerodynamics [1,5,23]. Again, it should be noted here that a normalization of the spacing with the upstream cylinder, as done in [5], would generally also be possible. In that case, individual vortex streets from the two cylinders would already be expected for several configurations with normalized spacings of $S/D = 2.7$ and 3.7. For example, for the cases with the thinnest upstream cylinder (diameter $d_u = 6$ mm), even the smallest normalized spacing of $S/D = 1.7$ would be in a regime where individual vortex shedding would be expected, as then $S/d_u = 8.5$ with $d_u = 6$ mm. Still, Fig. 9(a) and (d) do not show clear signs of distinct vortex shedding from the upstream cylinder.

Of course, the trend observed for small spacings and large ratios of d_d/d_u is not unexpected, as configurations with a small cylinder close to a thicker downstream cylinder can be expected to behave as one blunt body. According to [5], the flow in this regime is synchronized, in which the shear layers from the upstream cylinder reattach on the downstream

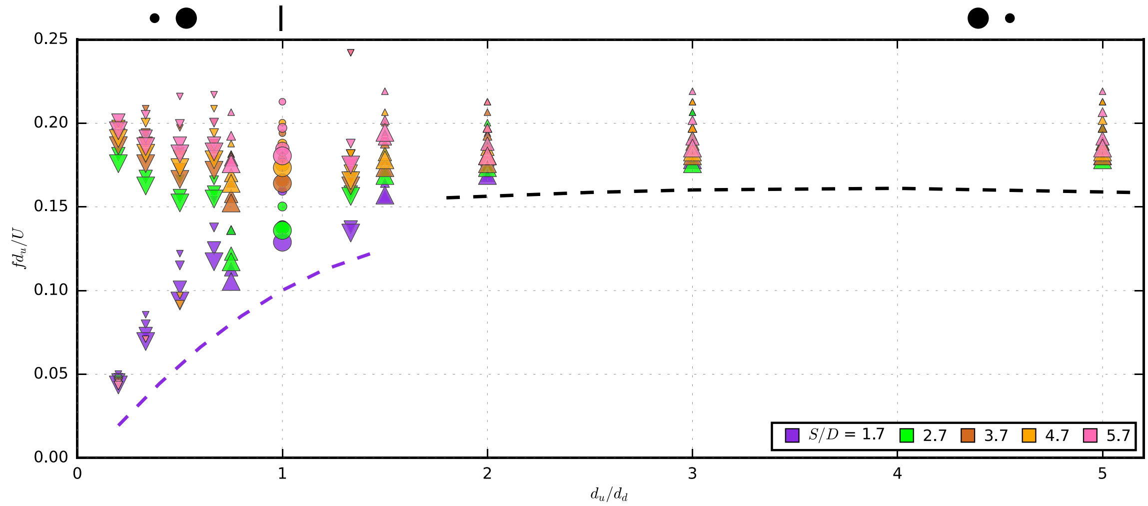

(a) Strouhal number based on upstream cylinder diameter as a function of d_u/d_d.

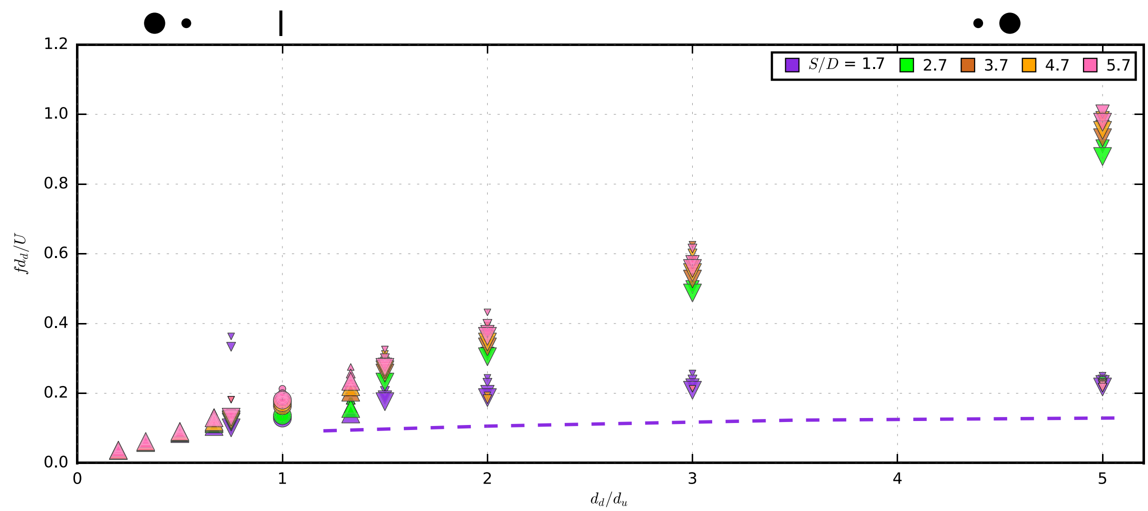

(b) Strouhal number based on downstream cylinder diameter as a function of d_d/d_u.

Fig. 8. Strouhal numbers as a function of cylinder diameter ratio (normalized spacings are color-coded, marker size increases with flow velocity, dashed black line indicates the region of approximately constant $f\,d_u/U$, dashed purple line indicates that of constant $f\,d_d/U$, ▼ $d_u/d_d < 1$, ● $d_u = d_d$, ▲ $d_u/d_d > 1$).

cylinder, which is clearly visible in Fig. 9(a) through (f). Interestingly, Fig. 8(b) also shows that the vortex shedding Strouhal number $f\,d_d/U$ for these configurations is not really constant, but slightly increases with increasing d_d/d_u. This could be due to the fact that in addition to the dependence of the Strouhal number on the Reynolds number [34,46,47] mentioned before, the fact that the upstream cylinder leads to notable turbulent inflow for the downstream cylinder also affects the vortex shedding [38,48].

3.3. Noise directivity

In this section, the effect of cylinder spacing and different cylinder diameters on the directivity of the vortex shedding tonal noise is briefly analyzed. To this end, Fig. 11 shows directivity plots of the amplitude of the tonal peak obtained by the microphones on the bottom arc in Fig. 1(b). Several observations can be made regarding the directivity of the vortex shedding tonal peak: Overall, the plots suggest a classical dipole noise directivity, which agrees well with theory for single circular cylinders [44] as well as with the observations made by Mg and Jothi [35], who deduced the dipole characteristics from the classical scaling with the sixth power of the free stream velocity. In addition, several configurations show a larger variability, meaning larger differences between curves for different diameter ratios at the same spacing, in the downstream region, e.g., at smaller angles. Examples are the configurations with S/D = 3.7 and 4.7 for the variation of the downstream cylinder (Fig. 11(f) and (h)). Although this is not visible for all configurations and hence could be caused by the differences between the configurations, it is also possible that this is additionally affected by the wind tunnel shear layers, whose effect on the amplitude of the sound waves has not been corrected in the current study.

4. Summary and conclusion

Tandem cylinder configurations are often used in aerodynamic and aeroacoustic studies, as they represent simple models for various applications such as the landing gear of aircraft. Several experimental studies exist for configurations where both cylinders have the same diameter, but very little data is available for configurations with two parallel cylinders of unequal diameter. In the study presented in the current paper, experiments were conducted on tandem cylinder configurations consisting of cylinders with diameters from 6 mm to 40 mm and normalized spacings (based on a nominal cylinder diameter of 30 mm)

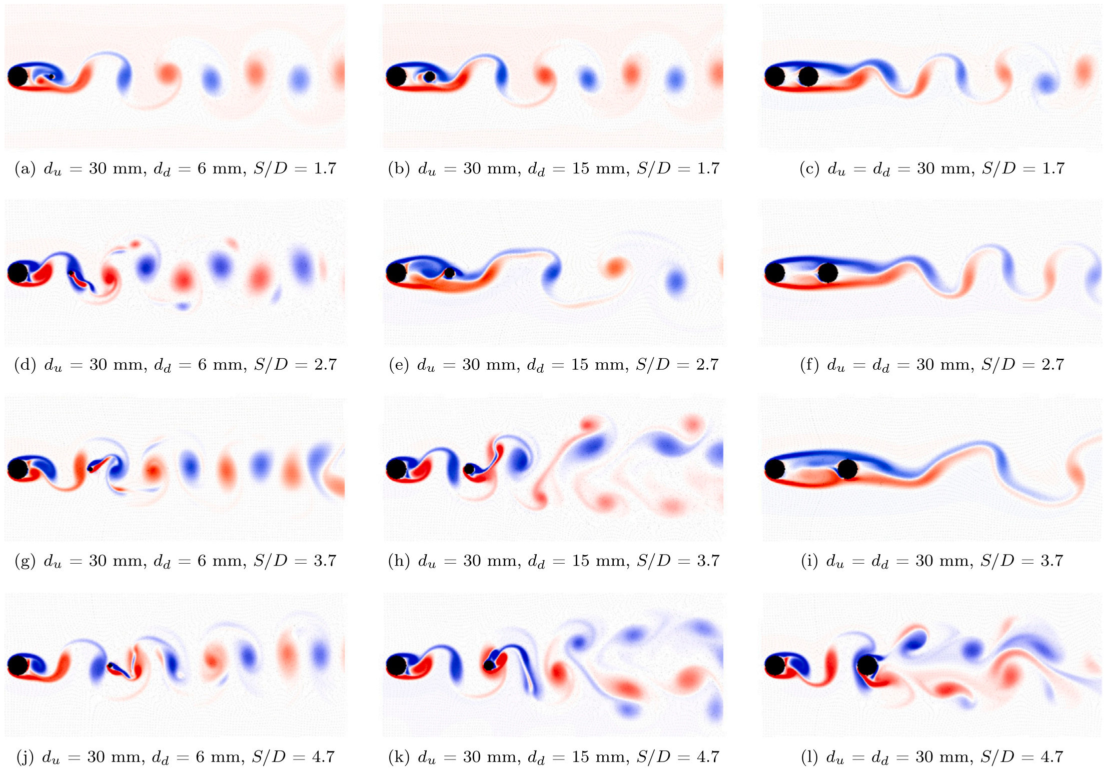

(a) $d_u = 30$ mm, $d_d = 6$ mm, $S/D = 1.7$ (b) $d_u = 30$ mm, $d_d = 15$ mm, $S/D = 1.7$ (c) $d_u = d_d = 30$ mm, $S/D = 1.7$

(d) $d_u = 30$ mm, $d_d = 6$ mm, $S/D = 2.7$ (e) $d_u = 30$ mm, $d_d = 15$ mm, $S/D = 2.7$ (f) $d_u = d_d = 30$ mm, $S/D = 2.7$

(g) $d_u = 30$ mm, $d_d = 6$ mm, $S/D = 3.7$ (h) $d_u = 30$ mm, $d_d = 15$ mm, $S/D = 3.7$ (i) $d_u = d_d = 30$ mm, $S/D = 3.7$

(j) $d_u = 30$ mm, $d_d = 6$ mm, $S/D = 4.7$ (k) $d_u = 30$ mm, $d_d = 15$ mm, $S/D = 4.7$ (l) $d_u = d_d = 30$ mm, $S/D = 4.7$

Fig. 9. Results from 2D flow simulations for configurations with larger or equal upstream cylinder diameters at selected spacings.

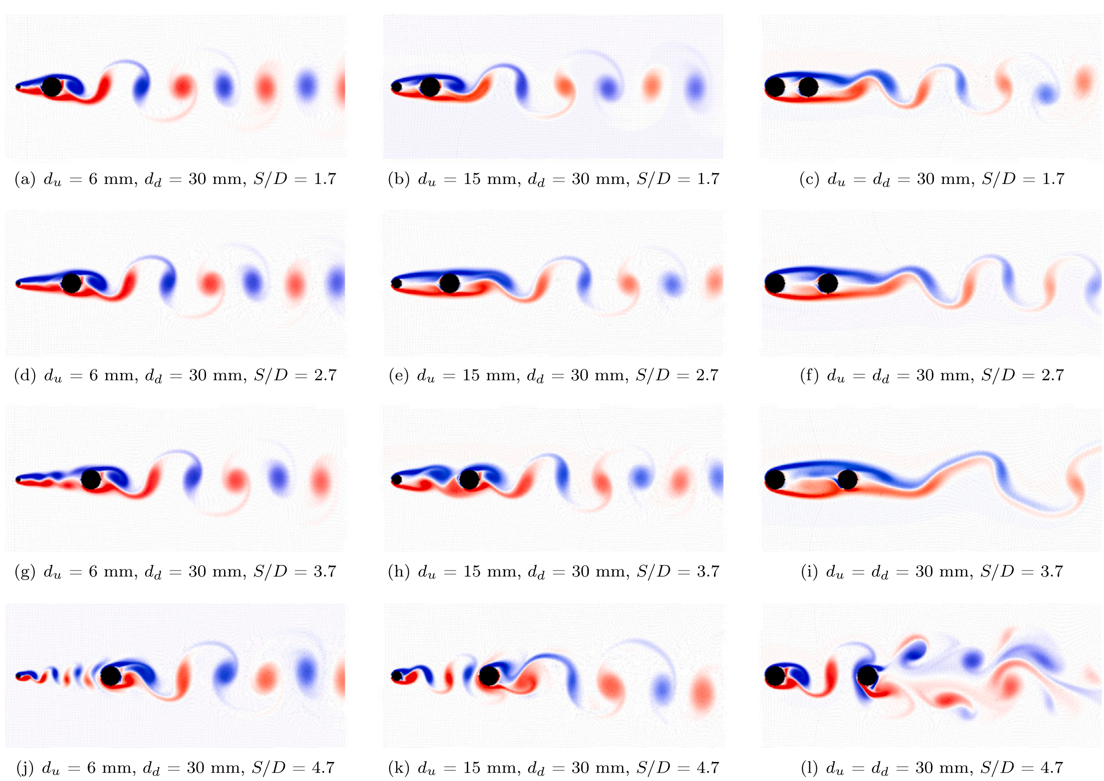

(a) $d_u = 6$ mm, $d_d = 30$ mm, $S/D = 1.7$ (b) $d_u = 15$ mm, $d_d = 30$ mm, $S/D = 1.7$ (c) $d_u = d_d = 30$ mm, $S/D = 1.7$

(d) $d_u = 6$ mm, $d_d = 30$ mm, $S/D = 2.7$ (e) $d_u = 15$ mm, $d_d = 30$ mm, $S/D = 2.7$ (f) $d_u = d_d = 30$ mm, $S/D = 2.7$

(g) $d_u = 6$ mm, $d_d = 30$ mm, $S/D = 3.7$ (h) $d_u = 15$ mm, $d_d = 30$ mm, $S/D = 3.7$ (i) $d_u = d_d = 30$ mm, $S/D = 3.7$

(j) $d_u = 6$ mm, $d_d = 30$ mm, $S/D = 4.7$ (k) $d_u = 15$ mm, $d_d = 30$ mm, $S/D = 4.7$ (l) $d_u = d_d = 30$ mm, $S/D = 4.7$

Fig. 10. Results from 2D flow simulations for configurations with larger or equal downstream cylinder diameters at selected spacings.

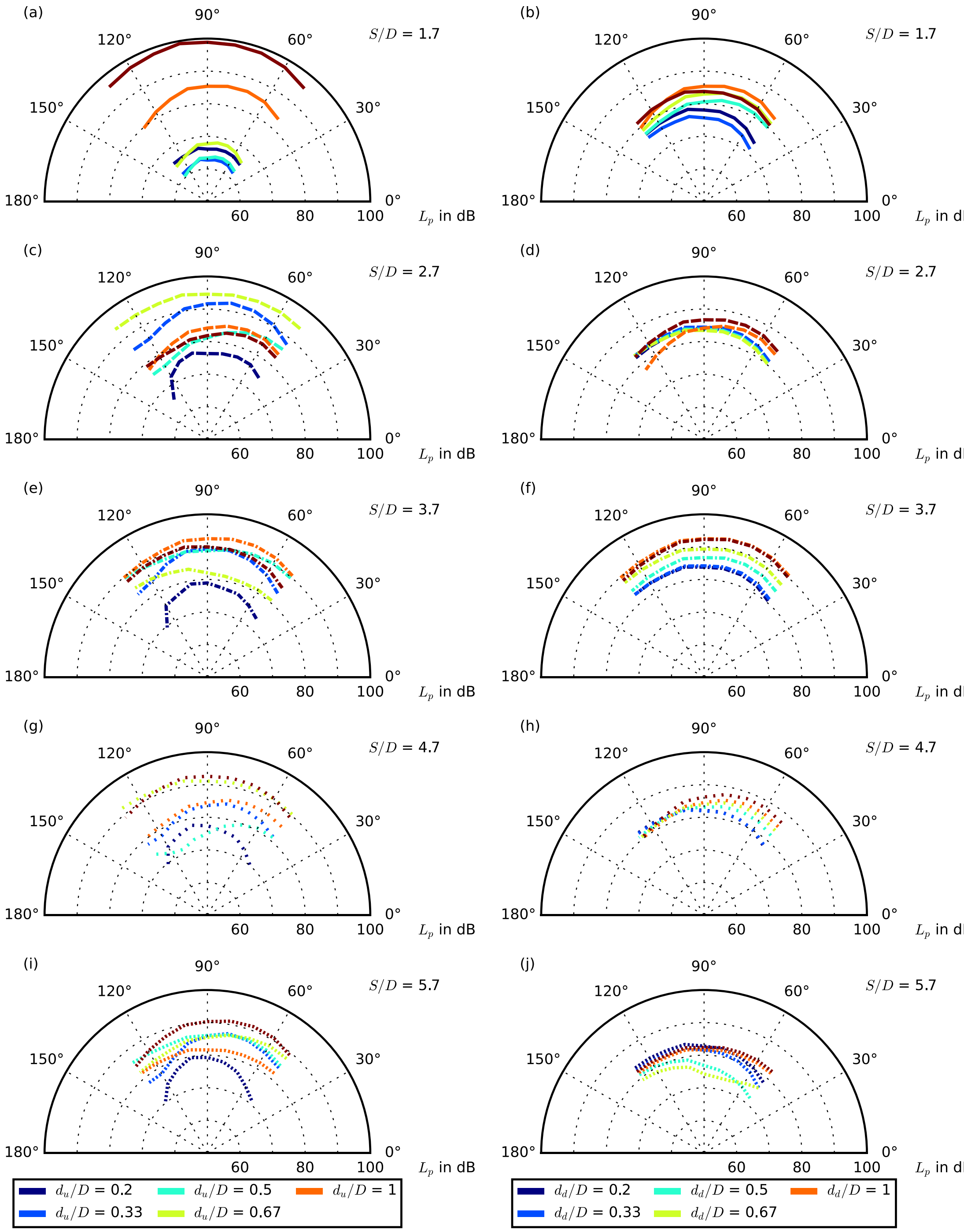

Fig. 11. Vortex shedding tonal noise directivities obtained at a flow speed of approximately 40 m/s ($M = 0.12$), left column: variation of the upstream cylinder diameter, right column: variation of the downstream cylinder diameter (flow from left to right).

S/D from 1.7 to 5.7 in an aeroacoustic wind tunnel. Acoustic measurements were performed using a set of free-field microphones and two-dimensional flow simulations were performed in order to provide qualitative flow visualizations.

The results show that for configurations where the upstream cylinder is thicker than the downstream cylinder, the vortex shedding seems to be governed by the upstream cylinder, basically across all spacings. For cases with a thinner upstream cylinder, there is not one distinct trend visible for all cylinder spacings. For small spacings, however, the vortex shedding periodicity scales with the downstream cylinder, which can be explained by the fact that the tandem cylinder configuration then acts as a single bluff body. These trends are confirmed by results from the set of flow simulations. The measured directivity of the dominating vortex shedding peak basically corresponds to an acoustic dipole, although for some configurations the upstream noise radiation is slightly increased compared to the downstream radiation. Another important finding is that even for large spacings, when two individual vortex shedding processes are visible in the flow simulations (and would be expected according to the literature), the far-field noise is still dominated by only a single tonal peak. This implies that not all periodic flow patterns observed in the vicinity of the cylinders are propagated into the far-field as sound. Thus, future research should aim at exploring the physics of the relation between the hydrodynamic near-field and the acoustic far-field of tandem cylinder configurations with unequal diameters in more detail.

The current paper presents an overview of a detailed aeroacoustic study on tandem cylinders with unequal diameters, with results that may be helpful for the design of low-noise technical applications as well as for the validation of computational fluid dynamics simulations. Several aspects of this research deserve additional attention, though, and may be a starting point for future experimental and/or numerical research.

CRediT authorship contribution statement

Thomas F. Geyer: Writing – original draft, Supervision, Project administration, Methodology, Formal analysis, Data curation, Conceptualization. **Paul Abromeit:** Writing – review & editing, Supervision, Investigation. **Maximilian Prügel:** Investigation, Formal analysis. **Sparsh Sharma:** Software, Writing – original draft. **Lars Enghardt:** Resources.

Declaration of competing interest

The authors declare that they have no known competing financial interests or personal relationships that could have appeared to influence the work reported in this paper.

Acknowledgments

The experimental work described in this paper was performed at the Brandenburg University of Technology as part of a student thesis. The authors thank Stefan Rohark (BTU Cottbus-Senftenberg) for his help with the experimental setup. This work made use of Flowsquare, a free two-dimensional computational fluid dynamics software.

Data availability

Data will be made available upon request.

References

[1] Zdravkovich MM. Flow induced oscillations of two interfering circular cylinders. J Sound Vib 1985;101(4):511–21. https://doi.org/10.1016/S0022-460X(85)80068-7
[2] Igarashi T. Characteristics of the flow around two circular cylinders arranged in tandem: 1st report. Bull. JSME 1981;24(188):323–31.
[3] Igarashi T. Characteristics of the flow around two circular cylinders arranged in tandem: 2nd report, unique phenomenon at small spacing. Bull. JSME 1984;27(233):2380–7.
[4] Hiwada M, Taguchi T, Mabuichi I, Kumada M. Fluid flow and heat transfer around two circular cylinders of different diameters in cross flow. Bull. JSME 1979;22(167):715–23. https://doi.org/10.1299/jsme1958.22.715
[5] Igarashi T. Characteristics of a flow around two circular cylinders of different diameters arranged in tandem. Bull. JSME 1982;25(201):349–57. https://doi.org/10.1299/jsme1958.25.349
[6] Zdravkovich MM. Flow around circular cylinders – volume 2: applications. vol. 2. Oxford University Press; 1997.
[7] Lockard D, Khorrami M, Choudhari M, Hutcheson F, Brooks TF, Stead D. Tandem cylinder noise predictions. In: 13th AIAA/CEAS aeroacoustics conference (28th AIAA aeroacoustics conference); 2007, AIAA paper 2007-3450. https://doi.org/10.2514/6.2007-3450
[8] Khorrami MR, Choudhari MM, Lockard DP, Jenkins LN, McGinley CB. Unsteady flowfield around tandem cylinders as prototype component interaction in airframe noise. AIAA J 2007;45(8):1930–41. https://doi.org/10.2514/1.23690
[9] Mussa A, Asinari P, Luo L-S. Lattice Boltzmann simulations of 2D laminar flows past two tandem cylinders. J Comput Phys 2009;228(4):983–99. https://doi.org/10.1016/j.jcp.2008.10.010
[10] Brès GA, Freed D, Wessels M, Noelting S, Pérot F. Flow and noise predictions for the tandem cylinder aeroacoustic benchmark. Phys Fluids 2012;24(3). https://doi.org/10.1063/1.3685102
[11] Weinmann M, Sandberg R, Doolan C. Tandem cylinder flow and noise predictions using a hybrid RANS/LES approach. Int J Heat Fluid Flow 2014;50:263–78. https://doi.org/10.1016/j.ijheatfluidflow.2014.08.011
[12] Maryami R, Ali SAS, Azarpeyvand M, Dehghan AA, Afshari A. The influence of cylinders in tandem arrangement on unsteady aerodynamic loads. Exp Therm Fluid Sci 2022;139:110709. https://doi.org/10.1016/j.expthermflusci.2022.110709
[13] Hu J, Zhou Y. Flow structure behind two staggered circular cylinders. Part 1. downstream evolution and classification. J Fluid Mech 2008;607:51–80. https://doi.org/10.1017/S0022112008001808
[14] Hu J, Zhou Y. Flow structure behind two staggered circular cylinders. Part 2. heat and momentum transport. J Fluid Mech 2008;607:81–107. https://doi.org/10.1017/S002211200800181X
[15] Sumner D, Richards MD, Akosile OO. Two staggered circular cylinders of equal diameter in cross-flow. J Fluids Struct 2005;20(2):255–76. https://doi.org/10.1016/j.jfluidstructs.2004.10.006
[16] Schewe G, van Hinsberg NP, Jacobs M. Investigation of the steady and unsteady forces acting on a pair of circular cylinders in crossflow up to ultra-high reynolds numbers. Exp Fluids 2021;62(8):176. https://doi.org/10.1007/s00348-021-03268-7
[17] Tong F, Cheng L, Zhao M. Numerical simulations of steady flow past two cylinders in staggered arrangements. J Fluid Mech 2015;765:114–49. https://doi.org/10.1017/jfm.2014.708
[18] Skonecki GM, Buick JM. Numerical study of flow around two circular cylinders in tandem, side-by-side and staggered arrangements. Fluids 2023;8(5):148. https://doi.org/10.3390/fluids8050148
[19] Mittal S, Kumar V. Flow-induced oscillations of two cylinders in tandem and staggered arrangements. J Fluids Struct 2001;15(5):717–36. https://doi.org/10.1006/jfls.2000.0376
[20] Papaioannou G, Yue D, Triantafyllou M, Karniadakis G. On the effect of spacing on the vortex-induced vibrations of two tandem cylinders. J Fluids Struct 2008;24(6):833–54. https://doi.org/10.1016/j.jfluidstructs.2007.11.006
[21] Griffith MD, Jacono DL, Sheridan J, Leontini JS. Flow-induced vibration of two cylinders in tandem and staggered arrangements. J Fluid Mech 2017;833:98–130. https://doi.org/10.1017/jfm.2017.673
[22] Assi GR. Wake-induced vibration of tandem cylinders of different diameters. J Fluids Struct 2014;50:329–39. https://doi.org/10.1016/j.jfluidstructs.2014.07.001
[23] Sumner D. Two circular cylinders in cross-flow: a review. J Fluids Struct 2010;26(6):849–99. https://doi.org/10.1016/j.jfluidstructs.2010.07.001
[24] Liu H, Azarpeyvand M, Wei J, Qu Z. Tandem cylinder aerodynamic sound control using porous coating. J Sound Vib 2015;334:190–201. https://doi.org/10.1016/j.jsv.2014.09.013
[25] Liu H, Wang Y, Wei J, Qu Z. The importance of controlling the upstream body wake in tandem cylinders system for noise reduction. Proc Inst Mech Eng G J Aerosp Eng 2018;232(3):517–31. https://doi.org/10.1177/0954410016682271
[26] Geyer TF. Experimental investigation of flow and noise control by porous coated tandem cylinder configurations. AIAA J 2022;60(7):4091–102. https://doi.org/10.2514/1.J061180
[27] Abromeit P, Geyer TF. Experimental assessment of the aerodynamic noise generated by a porous coated staggered tandem cylinder configuration. In: AIAA aviation forum and ascend 2025; 2025. https://doi.org/10.2514/6.2025-3214
[28] Zhou Y, Alam MM. Wake of two interacting circular cylinders: a review. Int J Heat Fluid Flow 2016;62:510–37. https://doi.org/10.1016/j.ijheatfluidflow.2016.08.008
[29] Geyer TF, Enghardt L. Noise generation by two staggered circular cylinders of equal diameter in cross-flow. In: 28th AIAA/CEAS aeroacoustics 2022 conference; 2022, AIAA paper 2022-3093. https://doi.org/10.2514/6.2022-3093
[30] Alam MM, Zhou Y. Strouhal numbers, forces and flow structures around two tandem cylinders of different diameters. J Fluids Struct 2008;24(4):505–26. https://doi.org/10.1016/j.jfluidstructs.2007.10.001
[31] Wang L, Alam MM, Zhou Y. Two tandem cylinders of different diameters in cross-flow: effect of an upstream cylinder on wake dynamics. J Fluid Mech 2018;836:5–42. https://doi.org/10.1017/jfm.2017.735
[32] Shan X. Effect of an upstream cylinder on the wake dynamics of two tandem cylinders with different diameters at low Reynolds numbers. Phys Fluids 2021;33(8). https://doi.org/10.1063/5.0060065
[33] Khan HH, Islam MD, Fatt YY, Janajreh I, Alam MM. Flow-induced vibration on two tandem cylinders of different diameters and spacing ratios. Ocean Eng 2022;258:111747. https://doi.org/10.1016/j.oceaneng.2022.111747
[34] Hutcheson FV, Brooks TF. Noise radiation from single and multiple rod configurations. Int J Aeroacoustics 2012;11(3–4):291–333. https://doi.org/10.1260/1475-472X.11.3-4.291
[35] Mg A, Jothi T. Aerodynamic noise characteristics of tandem cylinders in a subcritical flow regime. Proc Inst Mech Eng G J Aerosp Eng 2024;09544100241276063. https://doi.org/10.1177/09544100241276063
[36] Geyer TF, Abromeit P, Prügel M. Noise generation by tandem cylinders of different diameter in cross-flow. In: Proceedings of DAS|DAGA 2025. Deutsche Gesellschaft Für Akustik E. V.; 2025. p. 525–8. https://doi.org/10.71568/dasdaga2025.242
[37] Sarradj E, Fritzsche C, Geyer TF, Giesler J. Acoustic and aerodynamic design and characterization of a small-scale aeroacoustic wind tunnel. Appl Acoust 2009;70(8):1073–80. https://doi.org/10.1016/j.apacoust.2009.02.009
[38] Geyer TF, Lucius A, Schneider M, Enghardt L. Aerodynamic noise from circular cylinders under turbulent inflow conditions. AIAA J 2025;1–11.
[39] Sharma S, Geyer TF, Arcondoulis EJG. On the influence of porous coating thickness and permeability on passive flow and noise control of cylinders. J Sound Vib 2023;549:117563. https://doi.org/10.1016/j.jsv.2023.117563
[40] Porteous R, Moreau DJ, Doolan CJ. A review of flow-induced noise from finite wall-mounted cylinders. J Fluids Struct 2014;51:240–54. https://doi.org/10.1016/j.jfluidstructs.2014.08.012
[41] Schlichting H, Gersten K. Boundary-layer theory. 9th ed. Springer Verlag Berlin Heidelberg; 1997.
[42] Sarradj E, Herold G. A Python framework for microphone array data processing. Appl Acoust 2017;116:50–8. https://doi.org/10.1016/j.apacoust.2016.09.015

[43] Minamoto Y. Flowsquare 4.0: theory and computation. Http://flowsquare.com; 2013.
[44] Etkin B, Korbacher GK, Keefe RT. Acoustic radiation from a stationary cylinder in a fluid stream (aeolian tones). J. Acoust. Soc. Am. 1957;29(1):30–6. https://doi.org/10.1121/1.1908673
[45] Gennaro EM, Colaciti AK, Medeiros MA. On the controversy regarding the effect of flow shear on the strouhal number of cylinder vortex shedding. Aerosp Sci Technol 2013;29(1):313–20. https://doi.org/10.1016/j.ast.2013.04.002
[46] Roshko A. On the development of turbulent wakes from vortex streets. Tech. Rep 1191 NASA; 1954.
[47] Fey U, König M, Eckelmann H. A new strouhal–reynolds-number relationship for the circular cylinder in the range $47 < re < 2 \times 10^5$. Phys Fluids 1998;10(7):1547–9. https://doi.org/10.1063/1.869675
[48] Norberg C, Sundén B. Turbulence and reynolds number effects on the flow and fluid forces on a single cylinder in cross flow. J Fluids Struct 1987;1(3):337–57. https://doi.org/10.1016/0889-9746(87)90264-7